Computational Research Progress in Applied Science & Engineering
©PEARL publication, 2017

ISSN 2423-4591

CRPASE Vol. 03(01), 42-61, February 2017

Safety Assessment on Merge and Diverge Areas using Fuzzy Inference System, Artificial Neural Network, and Particle Swarm Optimization

Hamid Behbahani*, Sayyed Mohsen Hosseini, Alireza Taherkhani, Hemin Asadi

Department of Civil Engineering, Iran University of Science and Technology, P.O. Box 13114-16846, Tehran, Iran

Keywords

Safety level,
Near-crash events,
Diverge area,
Merge area,
Fuzzy inference system.

Abstract

In this paper, it was attempted to predict safety level of merge and diverge areas by simulating 2880 different types of them with different geometry and traffic characteristics. After analyzing trajectory data, safety level was obtained for each merge and diverge area by defining an index called "No-Collision Potential Index". This index depends on the number and severity of near-crash events and could be determined by combining four traffic conflict techniques using fuzzy inference system. A database containing geometric and traffic characteristics as variables and safety level as function was generated after determination of safety level for all types of merge and diverge areas. By using this database, two models were developed to predict safety level of the two areas, one by artificial neural network and another using particle swarm optimization algorithm. Models were tested, validated and their errors were checked. The results indicated good accuracy of similarity between the results of models in predicting safety level of merge and diverge areas and that of simulations. Five merge areas and five diverge areas as case studies were surveyed to verify the models. Statistical analysis showed that there was no significant difference between means of safety level predicted by models and safety level obtained from case studies.

1. Introduction

Providing an acceptable Safety Level (*SL*) of traffic facilities is vital due to its consequential effects on prevention of fatality and property damage. Freeways have always played an important role in road transportation. Hence, the *SL* in freeways has been one of the main concerns of researchers. Every freeway should have a continuous high-speed flow along with a high *SL*. Operation of freeways has been always affected by operation of merge and diverge areas. *SL* is a common criterion which represents the quality of operation in these areas. In this paper, it was attempted to develop some models to predict *SL* of merge and diverge areas according to their traffic and geometric characteristics. To do this, *SL* for a specific merge area and a specific diverge area with specific traffic and geometric characteristics was calculated based on trajectory data using simulation. By combining four traffic conflict techniques using Fuzzy Inference System (FIS) and finally by defining an index called "No-Collision Potential Index" (*NCPI*), the *SL* was determined. By changing traffic and geometric characteristics of the merge and diverge areas, 2160 types of merge areas and 720 types of diverge areas were produced. *SL* was determined for every type using simulation and analyzing trajectory data. Thus, a database was generated with 2160 rows of information for merge areas which contain seven traffic and geometric variables and one function of *SL* and 720 rows of information for diverge areas which contain six traffic and geometric variables and one function of *SL*. These rows of information were used to develop the models. First model was developed by Artificial Neural Network (*ANN*) and second by Particle Swarm Optimization (*PSO*) algorithm that both are illustrated in future sections. After checking the accuracy of models, case studies were used to verify them.

2. Literature Review

Safety aspects of different segments of freeways were highly considered in previous researches. Since the operation of merge and diverge areas directly affects the performance of freeways, several studies were conducted on assessment or prediction of safety of these areas and effective factors on their safety were investigated. Xie et al. [1] stated that parallel-type single-lane exit ramp are safer than taper-type

* Corresponding Author:
E-mail address: behbahani@iust.ac.ir– Tel, (+98) 9196075121

Received: 12 October 2016; Accepted: 28 January 2017

single-lane exit ramp by analyzing 10 Single-lane Right Exit Ramp on Freeways of China. Eustace et al. [2] used a four-year record of crash data (2005–2008) and a statistical modeling technique that assumes a negative binomial distribution on generalized linear models to develop separate models for merging and diverging areas. Their model results showed that left-side merging and diverging areas are critical elements in crash frequency in the vicinity of ramps on freeways. their results also indicated that crashes are about 7.88 times more likely to occur on merging areas located on the left side of the freeway lanes compared to those on the right. For diverging areas, about 2.26 times more crashes are likely to occur near diverging areas on the left compared to those diverging on the right side of the freeway. Chen et al. in 2011 [3] studied crash records at a total of 11 left-side and 63 similar right-side diverge areas in Florida. They found that the left-side off-ramp had higher average crash counts, crash rate and percentage of severe crashes. Higher number of lanes on freeways, higher number of lanes on ramps, and speeding related crashes tend to increase the likelihood of sustaining severe injuries at freeway merging locations. speeding related crashes and angle-type collisions increase the likelihood of severe injury crashes at diverging areas [4]. Sarvi [5] investigated traffic behavior and characteristics during the merging process under congested situations in order to design safer and less congested merging points as well as to apply more efficient control at these bottleneck sections by a three-year extensive study. The results show that aggressive and avoidance lane-changing restriction strategies decrease potential conflicts between vehicles. Lu et al. [6] investigated a three-years crash data from 282 freeway exit ramps and Three types of crashes consist of rear-end, sideswipe, and angle collisions were considered during their investigation. multivariate Poisson-lognormal model was estimated to jointly evaluate the impacts of explanatory variables on different collision risks. They reported that rear-end and angle collisions were likely to result in more severe outcomes as compared to the sideswipe collisions. Kiattikomol et al. [7] developed practical tools for assessing safety consequences of freeways in the context of long-range urban transportation plans. The researchers used the negative-binomial regression modeling approach to develop separate models to predict the number of crashes for different levels of crash severity for non-interchange segments, and interchange segments, respectively. They presented crash prediction models, which can be used by metropolitan planning organizations planners to evaluate the safety impact of alternative freeway networks when comparing their costs and benefits in the long-range planning context. In order to be in the safe state, the driver of the diverging car must know the critical distance (below which the way out will be out of his reach) in each lane. This critical distance depends on the density of cars, and it follows an exponential law [8]. Study on interchanges along Highways to quantify the effects of ramp terminal spacing and traffic volumes on safety performance was done and statistically significant models relating factors such as traffic volumes and geometric features to collision frequency were developed. It was found that:

The results of collision modelling using four different exposure approaches indicated that the exponential relationship between a single exposure term and the collision frequency resulted in the best model fit and was hence included along with other combinations of explanatory variables in all developed models. Increasing the number of vehicles that enter and exit the freeway at a specific segment would cause an increase in the number of collisions on this segment. The general trend of the relationship between the length of the speed change lane and the collision frequency of the associated segment suggests decreasing number of collisions with increasing the length of speed change lane. Carrying the full width of the speed change to the gore of the following ramp might increase the number of collisions on the segment between these two ramps. Therefore, it is recommended to provide the speed change lane with a tapered portion at the end and beginning of acceleration and deceleration lanes, respectively. In cases that warrant an increase or decrease in the basic number of lanes to satisfy the capacity needs of the freeway, extending the speed change lane is not recommended. Alternatively, changing the number of lanes should be implemented within the basic section and away from the influence of speed change lanes. Off- ramps with design criteria that provide relatively high speeds for vehicles exiting the freeway would allow safer operational conditions compared to off-ramps with relatively lower speeds [9].

Different techniques for Surrogate Safety Measures (*SSM*) such as Time-To-Collision (*TTC*), Post Encroachment Time (*PET*), Proportion of Stopping Distance (*PSD*), Crash Potential Index (*CPI*), Unsafe Density (*UD*), Max Speed (Max *S*), Relative Speed (Δv), Kinetic Energy (*KE*), and Deceleration Rate to Avoid Collision (*DRAC*) were defined by previous researchers to estimate the danger or risk of collision. Four of these techniques have been chosen in this paper due to similarity between the objectives. Definitions of *TTC*, *DRAC*, *KE*, and Δv in *SSM* are presented in following paragraphs.

TTC: *TTC* was defined first by Hayward as the remaining collision occurrence time between two vehicles if collision course and speed difference maintained constant [10]. When *TTC* is low, there is an imminent danger of collision [11]. *TTC* for rear-end conflicts can be calculated by Eq. (1) [12].

$$TTC_F(t) = \frac{X_L(t) - X_F(t) - l_L}{V_F(t) - V_L(t)} \qquad \forall V_F(t) > V_L(t) \qquad (1)$$

where *TTC* is the Time-to-collision, *X* is the vehicle position (L: leading and F: following), *V* is the vehicle speed (*L*: leading and *F*: following), and *l* is the vehicle length.

DRAC: Deceleration rate is a good measure to detect dangerous maneuvers. *DRAC* is the rate at which a vehicle must decelerate to avoid a probable collision. For vehicles, travelling in the same path *DRAC* is [13]

$$DRAC_t = \frac{(V_{F(t)} - V_{L(t)})^2}{2[(X_{L(t)} - X_{F(t)}) - l_{veh\ L}]} \qquad (2)$$

in which $L_{veh\ L}$ is the length of leading vehicle and other parameters were described previously.

For angled conflicts the equation changes as follows

$$DRAC_t = \frac{\Delta V_{ij(t)}{}^2}{2\, D_{i(t)}} \qquad (3)$$

where $\Delta V_{ij(t)}$ is relative speed of two vehicle engaged in conflict and $D_{i(t)}$ is the distance between the current position of the vehicle i and point of intersection ahead of two vehicles.

KE: From Newtonian physics, we know that a moving vehicle has a kinetic energy as Eq. (4) [2]

$$K = \frac{1}{2}mv^2 \quad (4)$$

where *K* is kinetic energy, m is mass, and v is speed of vehicle. The kinetic energy transferred to the target vehicle can be calculated from Eq. (5)

$$KE_s = \frac{1}{2}.m_s.\Delta {v_s}^2 \quad (5)$$

in which KE_s is the kinetic energy transferred to the target vehicle, m_s is the mass of target vehicle, and Δv_s is the change of the target vehicle speed before and after the collision [14].

Δv: *Δv* is the relative speed of vehicles involved in the conflict as long as collision severity reflector [15].

Behbahani and Nadimi [16] presented a new framework to calculate the risk of sideswipe collisions instantaneously based on *SSM*. Behbahani et al. [17] also developed a new application of *TTC* for enhancement of road safety assessment in their study. Values for both rate of *TTC* variation and the level of hazard associated by *TTC* have been amalgamated as an approximate safety indicator. The proposed technique for collision prediction is shown to provide a more accurate level of risk assessment with respect to car-following scenarios.

3. Model Development

By using trajectory data, in this paper, it was attempted to develop a model to predict *SL* of merge and diverge areas based on geometry and traffic characteristics of these areas. *SL* was obtained by defining an index called *NCPI*. *NCPI* is a quantitative index based on the number and severity of possible collisions in the study area. The value of *NCPI* is in the range of zero to 100. The higher the value of *NCPI*, the higher the *SL*.

Traffic conflict techniques including *TTC*, *DRAC*, *KE*, and *ΔV* were employed to determine *NCPI*. Number of possible collision were predicted using *TTC* and *DRAC* and severity of these collisions were predicted by *KE* and *ΔV*.

Merge and diverge areas with different geometric and traffic characteristics, simulated, and coordinates of vehicles at intervals of 0.1 seconds were extracted during simulation.

It should be noted that any collision in merge or diverge areas could be a rear-end collision or occurs at an angle of β. Thus, analysis should be done with respect to angled collisions. In a special case which the angle of collision is zero, it will be a rear-end collision. Collision of two vehicles at an angle of *β* is described in Figure 1.

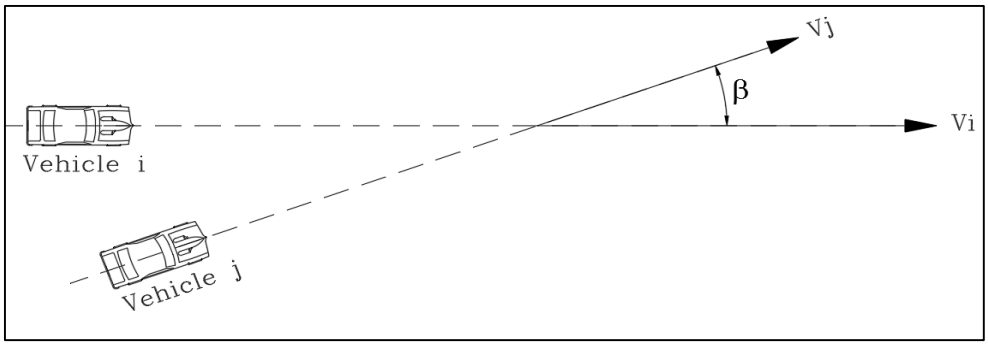

Figure 1. Collision of two vehicles at an angle of *β*

In this paper, it was assumed that the movement of vehicles is linear and with a constant acceleration or deceleration. So, the coordinates of intersection ahead of two vehicles *i* and *j* could be computed. Acceleration or deceleration rate and speed of vehicles could be determined using these assumptions. It is necessary to check whether the coordinates of intersection ahead of two vehicles is within the limits of merge or diverge area or not. By assuming no changes in the conditions, it can be concluded that two vehicles *i* and *j* will never collide with each other if the coordinates is outside of the limits of study area.

The distance between the position of each vehicle to the intersection ahead and the time required to reach this point can be obtained as follows. Here, it was assumed that vehicle *i* reach the point of intersection before vehicle *j*.

$$L_{ij} = [(x_c - x_{i1})^2 + (y_c - y_{i1})^2]^{0.5} \quad (6)$$

$$L_{ij} = 0.5a_i\ {T_i}^2 + V_i\,T_i \quad \Rightarrow \quad T_i = \left[\left(\frac{{a_i}^2}{4} + 2a_iL_{ij}\right)^{0.5} - V_i\right]/a_i \quad (7)$$

$$L_{ji} = \left[(x_c - x_{j1})^2 + (y_c - y_{j1})^2\right]^{0.5} - L_{Veh\,i}\ cos\,\beta \quad (8)$$

$$L_{ji} = 0.5a_j{T_j}^2 + V_jT_j \quad \Rightarrow \quad T_j = \left[\left(\frac{{a_j}^2}{4} + 2a_jL_{ji}\right)^{0.5} - V_j\right]/a_j \quad (9)$$

In which L_{ij} and L_{ji} are the distance between the position of vehicles i and j to the intersection ahead. x_c and y_c are the coordinates of intersection ahead. x_{i1} and y_{i1} are the coordinates of vehicle i and x_{j1} and y_{j1} are the coordinates of vehicle *j* at the time of t_1. a_i and a_j are acceleration or deceleration rate of vehicles *i* and *j*, and V_i and V_j are speed of vehicles *i* and *j* at the time of t_1, respectively. T_i and T_j are the time required to reach the point of intersection for vehicles *i* and *j*, respectively. $L_{Veh\,i}$ is the length of vehicle *i*.

While the absolute value of the difference of T_i and T_j is less than the critical time to collision, there will be a near-crash event. The value of critical time to collision varies in several studies but the value of 5 seconds had the highest frequency [18-20].

Among different couples of vehicles *i* and *j*, the number of those that are encountered a near-crash event were counted as Eq. (10)

$$C_{TTC} = Count_i^j \left[\left|T_i - T_j\right| < TTC_{critical}\right] \quad (10)$$

in which C_{TTC} is the number of couples of vehicles that are encountered a near-crash event. With respect to the angled collision of two vehicles *i* and *j*, the relative speed of these two vehicles at the time of collision could be determined as follows in each directions of vehicles *i* and *j*.

$$\Delta V_{ij} = V_i - V_j \cos\beta \quad (11)$$

$$\Delta V_{ji} = V_j - V_i \cos\beta \quad (12)$$

in which β is the angle of collision. Minimum *DRAC* could be also found by Eq.s (13) and (14).

$$DRAC_{ij} = 0.5\, \Delta V_{ij}{}^2\, L_{ij}{}^{-1} \quad (13)$$

$$DRAC_{ji} = 0.5\, \Delta V_{ji}{}^2\, L_{ji}{}^{-1} \quad (14)$$

Maximum *DRAC* for every vehicles was proposed by Maurya and Bokare [21]. So, if the value of each of the *DRAC*s is more than the maximum *DRAC*, there will be a near-crash event. The *DRAC* of a couple of vehicles i and j is the maximum *DRAC* of them. The number of cases in which a near-crash event takes place, will be counted by Eq. (16)

$$DRAC = max\{DRAC_{ij}\,.\,DRAC_{ji}\} \quad (15)$$

$$C_{DRAC} = Count_i^j \left[DRAC > DRAC_{Max}\right] \quad (16)$$

in which C_{DRAC} is the number of cases in which a near-crash event occurs. The speed of vehicle *i* at the time of collision is calculated by Eq. (17).

$$V_{i-collision} = a_i \times T_i + V_i \quad (17)$$

Decomposition of speed vectors at the moment of collision is shown in Figures 2 and 3.

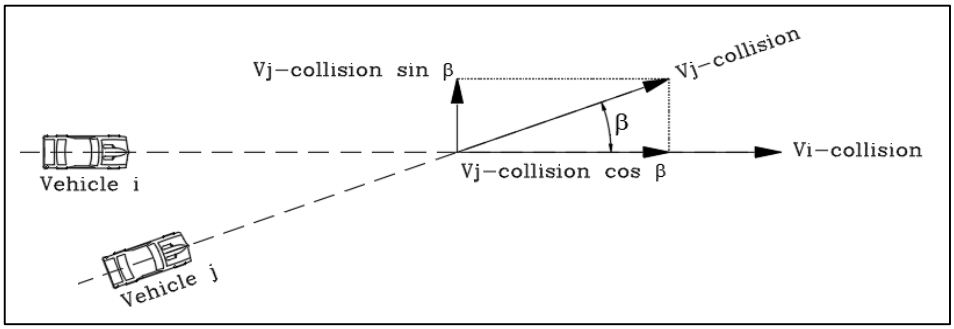

Figure 2. Decomposition of speed vectors of vehicl *j* parallel with and perpendicular to the movement direction of vehicl *i.*

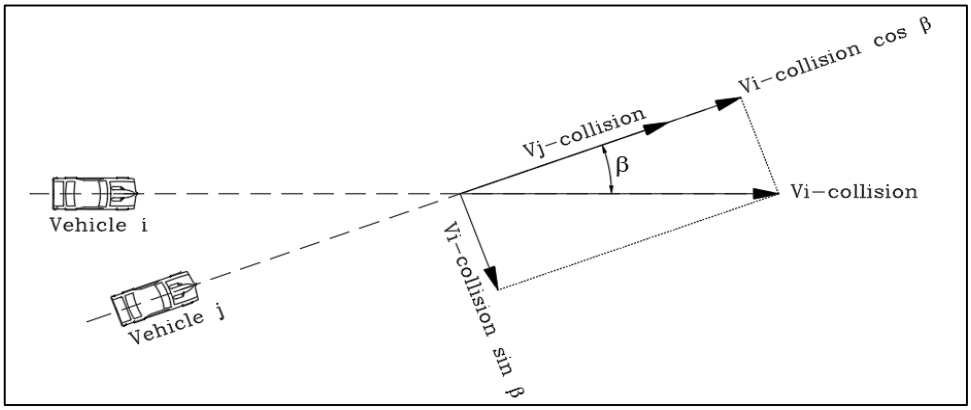

Figure 3. Decomposition of speed vectors of vehicl *i* parallel with and perpendicular to the movement direction of vehicl *j*

So, the relative speed of two vehicles *i* and *j* at themoment of collision could be determined by Eq. (19).

$$\overrightarrow{\Delta V} = \overrightarrow{\Delta V_{i-parallel}} + \overrightarrow{\Delta V_{i-perpendicular}} = \overrightarrow{\Delta V_{J-parallel}} + \overrightarrow{\Delta V_{J-perpendicular}} \quad (18)$$

$$\Delta V = \left|\overrightarrow{\Delta V}\right| = \left[\left|\overrightarrow{\Delta V_{i-parallel}}\right|^2 + \left|\overrightarrow{\Delta V_{i-perpendicular}}\right|^2\right]^{0.5} = \left[\left|\overrightarrow{\Delta V_{J-parallel}}\right|^2 + \left|\overrightarrow{\Delta V_{J-perpendicular}}\right|^2\right]^{0.5} \quad (19)$$

$$\left|\overrightarrow{\Delta V_{i-parallel}}\right| = \left|\overrightarrow{V_{i-collision}}\right| - \left|\overrightarrow{V_{J-collision}}\right| \cos\beta \quad (20)$$

$$\left|\overrightarrow{\Delta V_{i-perpendicular}}\right| = \left|\overrightarrow{V_{J-collision}}\right| \sin\beta \quad (21)$$

$$\left|\overrightarrow{\Delta V_{J-parallel}}\right| = \left|\overrightarrow{V_{J-collision}}\right| - \left|\overrightarrow{V_{i-collision}}\right| \cos\beta \quad (22)$$

$$\left|\overrightarrow{\Delta V_{J-perpendicular}}\right| = \left|\overrightarrow{V_{i-collision}}\right| \sin\beta\,. \quad (23)$$

If the difference of speed of vehicle *j* before and after the collision is equal to the ΔV obtained above, the amount of kinetic energy transferred in the collision, will be defined as follows.

$$KE_{ij} = 0.5\, m_j \Delta V^2 \quad (24)$$

In which m_j is the mass of vehicle j.

Four traffic conflict techniques were used to predict number and severity of possible collisions. But the probability that a near-crash event becomes a real collision should be determined and considered in model development. There are two following probabilities:

1. The probability that after detection of an event as a near-crash event, the event becomes a real collision (It is possible that both or one of the drivers prevent(s) collision to take place by changing speed, direction, or path).

2. The probability that severity of collision does not change (It is possible that both or one of the drivers engaged in a collision reduce(s) their (his) speed to avoid collision if there is time. Even if the collision occurs, the collision severity will become lower).

There will be both above probabilities, when there is time for reaction of drivers. In the other words, the more time to collision, the less probability of taking place the collision with certain severity. The Probability Density Function (PDF) should be sensitive to minimum reaction time of drivers, too. Thus, an exponential *PDF* was selected to satisfy the requirements of the problem which could be written as Eq. (25)

$$Pr_i = \lambda e^{-\lambda(0.5\ TTC_i^2\ t_{reaction}^{-2})} \quad (25)$$

in which Pr_i is the probability that a near-crash event with certain severity becomes a real collision with that severity, $t_{reaction}$ is reaction time of drivers and λ is a constant value which should be defined based on the problem. When avoiding a collision requires changes in speed, path, or direction, AASHTO recommends a range of reaction time between 10.2 to 11.2 seconds in freeway [22]. Since the probability must close to 1.0 when *TTC* approaches zero seconds, the value of λ should be equal to 1.0. Figure 4 presents variation of probability that a near-crash event becomes a real collision against *TTC* with $\lambda=1$ and $t_{reaction}=11.2$.

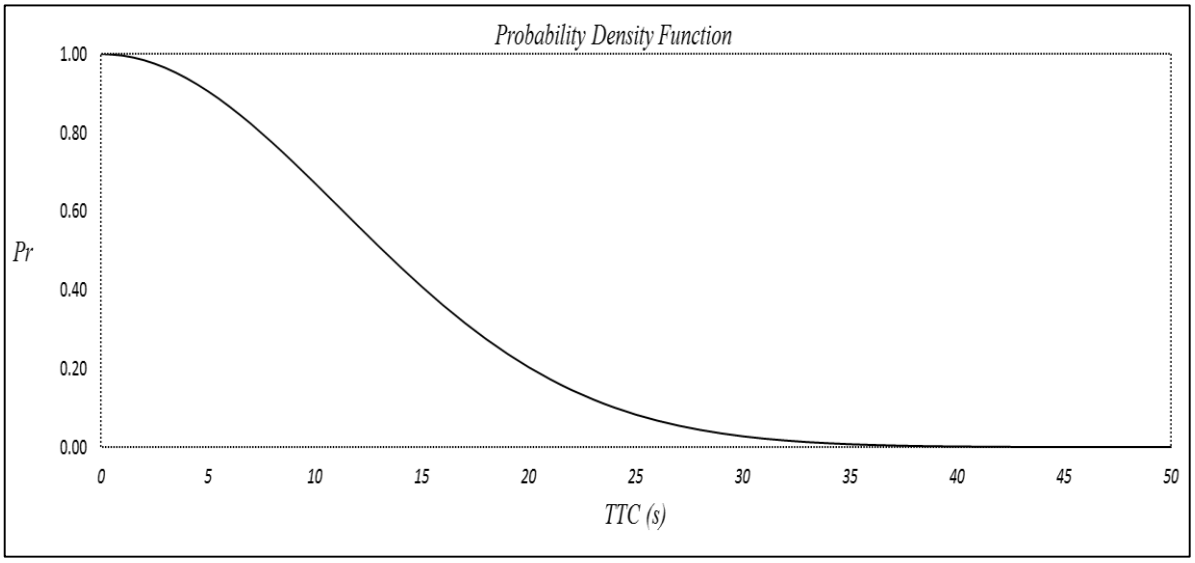

Figure 4. *PDF* for a near-crash event becomes a real collision

Number and severity of collisions in merge and diverge areas could be better predicted by applying the above probability as Eq.s (26) to (29)

$$N_{TTC} = {C_{TTC}}^{-1} \times \sum_{i=1}^{C_{TTC}} Pr_i\, C_{TTC\,i} \quad (26)$$

$$N_{DRAC} = {C_{DRAC}}^{-1} \times \sum_{i=1}^{C_{DRAC}} Pr_i\, C_{DRAC\,i} \quad (27)$$

$$S_{KE} = {C_{TTC}}^{-1} \times \sum_{i=1}^{C_{TTC}} (Pr_i \times KE_i) \quad (28)$$

$$S_{\Delta V} = {C_{TTC}}^{-1} \times \sum_{i=1}^{C_{TTC}} (Pr_i \times \Delta V_i) \quad (29)$$

in which N_{TTC} is predicted number of collisions by *TTC* technique, N_{DRAC} is predicted number of collisions by *DRAC* technique, S_{KE} is predicted collisions severity by *KE* technique, and $S_{\Delta V}$ is predicted collisions severity by ΔV technique. But the results of predicted number of collisions using *TTC* and *DRAC* techniques were different and the results of predicted severity of collisions using *KE* technique were not the same as those by ΔV technique, as well. But all results are considerable and could be correct. So, all the results from four techniques should be considered together to define *NCPI*. In the other words, *NCPI* is a function of the results of four mentioned techniques as four variables as Eq. (30).

$$NCPI = F(N_{TTC}\,.N_{DRAC}\,.S_{KE}\,.S_{\Delta V}) \quad (30)$$

Determining function of *NCPI* was defined using Fuzzy Inference System (*FIS*). In this way, the quantitative results of four techniques were changed into qualitative results using fuzzification. For this purpose, the quantitative value of each variable was automatically placed in three qualitative group of low, medium, and high after fuzzification.

The rules of *FIS* between *NCPI* and its variables were set and therefore *NCPI* would be obtained in qualitative form in five group of very low, low, medium, high, and very high. Table 1 describes the applied rules of *FIS*.

Table 1. The rules of *FIS*

Rule NO.	Variables				Function
	$S_{\Delta V}^{-1}$	S_{KE}^{-1}	N_{ttc}^{-1}	N_{drac}^{-1}	*NCPI*
1	Low	Low	Low	Low	Very Low
2	Low	Low	Low	Medium	Very Low
3	Low	Low	Low	High	Low
4	Low	Low	Medium	Low	Very Low
5	Low	Low	Medium	Medium	Low
6	Low	Low	Medium	High	Medium
7	Low	Low	High	Low	Low
8	Low	Low	High	Medium	Medium
9	Low	Low	High	High	High
10	Low	Medium	Low	Low	Very Low
11	Low	Medium	Low	Medium	Low
12	Low	Medium	Low	High	Medium
13	Low	Medium	Medium	Low	Low
14	Low	Medium	Medium	Medium	Medium
15	Low	Medium	Medium	High	Medium
16	Low	Medium	High	Low	Medium
17	Low	Medium	High	Medium	Medium
18	Low	Medium	High	High	High
19	Low	High	Low	Low	Low
20	Low	High	Low	Medium	Medium
21	Low	High	Low	High	Medium
22	Low	High	Medium	Low	Medium
23	Low	High	Medium	Medium	Medium
24	Low	High	Medium	High	High
25	Low	High	High	Low	Medium
26	Low	High	High	Medium	High
27	Low	High	High	High	Very High
28	Medium	Low	Low	Low	Very Low
29	Medium	Low	Low	Medium	Low
30	Medium	Low	Low	High	Low
31	Medium	Low	Medium	Low	Low
32	Medium	Low	Medium	Medium	Low
33	Medium	Low	Medium	High	Medium
34	Medium	Low	High	Low	Low
35	Medium	Low	High	Medium	Medium
36	Medium	Low	High	High	High
37	Medium	Medium	Low	Low	Low
38	Medium	Medium	Low	Medium	Low
39	Medium	Medium	Low	High	Medium
40	Medium	Medium	Medium	Low	Low
41	Medium	Medium	Medium	Medium	Medium
42	Medium	Medium	Medium	High	High
43	Medium	Medium	High	Low	Medium
44	Medium	Medium	High	Medium	High
45	Medium	Medium	High	High	Very High
46	Medium	High	Low	Low	Low
47	Medium	High	Low	Medium	Medium
48	Medium	High	Low	High	High
49	Medium	High	Medium	Low	Medium
50	Medium	High	Medium	Medium	High
51	Medium	High	Medium	High	High
52	Medium	High	High	Low	High
53	Medium	High	High	Medium	High
54	Medium	High	High	High	Very High
55	High	Low	Low	Low	Very Low
56	High	Low	Low	Medium	Low
57	High	Low	Low	High	Medium
58	High	Low	Medium	Low	Low
59	High	Low	Medium	Medium	Medium
60	High	Low	Medium	High	High
61	High	Low	High	Low	Medium
62	High	Low	High	Medium	High
63	High	Low	High	High	High
64	High	Medium	Low	Low	Low

Rule NO.	Variables				Function
	$S_{\Delta V}^{-1}$	S_{KE}^{-1}	N_{ttc}^{-1}	N_{drac}^{-1}	*NCPI*
65	High	Medium	Low	Medium	Medium
66	High	Medium	Low	High	Medium
67	High	Medium	Medium	Low	Medium
68	High	Medium	Medium	Medium	Medium
69	High	Medium	Medium	High	High
70	High	Medium	High	Low	Medium
71	High	Medium	High	Medium	High
72	High	Medium	High	High	Very High
73	High	High	Low	Low	Medium
74	High	High	Low	Medium	Medium
75	High	High	Low	High	High
76	High	High	Medium	Low	Medium
77	High	High	Medium	Medium	High
78	High	High	Medium	High	Very High
79	High	High	High	Low	High
80	High	High	High	Medium	Very High
81	High	High	High	High	Very High

Then quantitative value of *NCPI* could be determined using Defuzzification. Default of *FIS* for determination of *NCPI* are presented in Table 2.

Figures 5 to 8 show the *FIS* structure and properties separately for merge and diverge areas.

Table 2. Default of *FIS* for determination of *NCPI*

Type	mamdani
Inputs/Outputs	[4 1]
Number of Input MFs	[3 3 3 3]
Number of Output MFs	5
Number of Rules	81
And Method	min
Or Method	max
Imp Method	min
Aggregate Method	max
Defuzzification Method	centroid

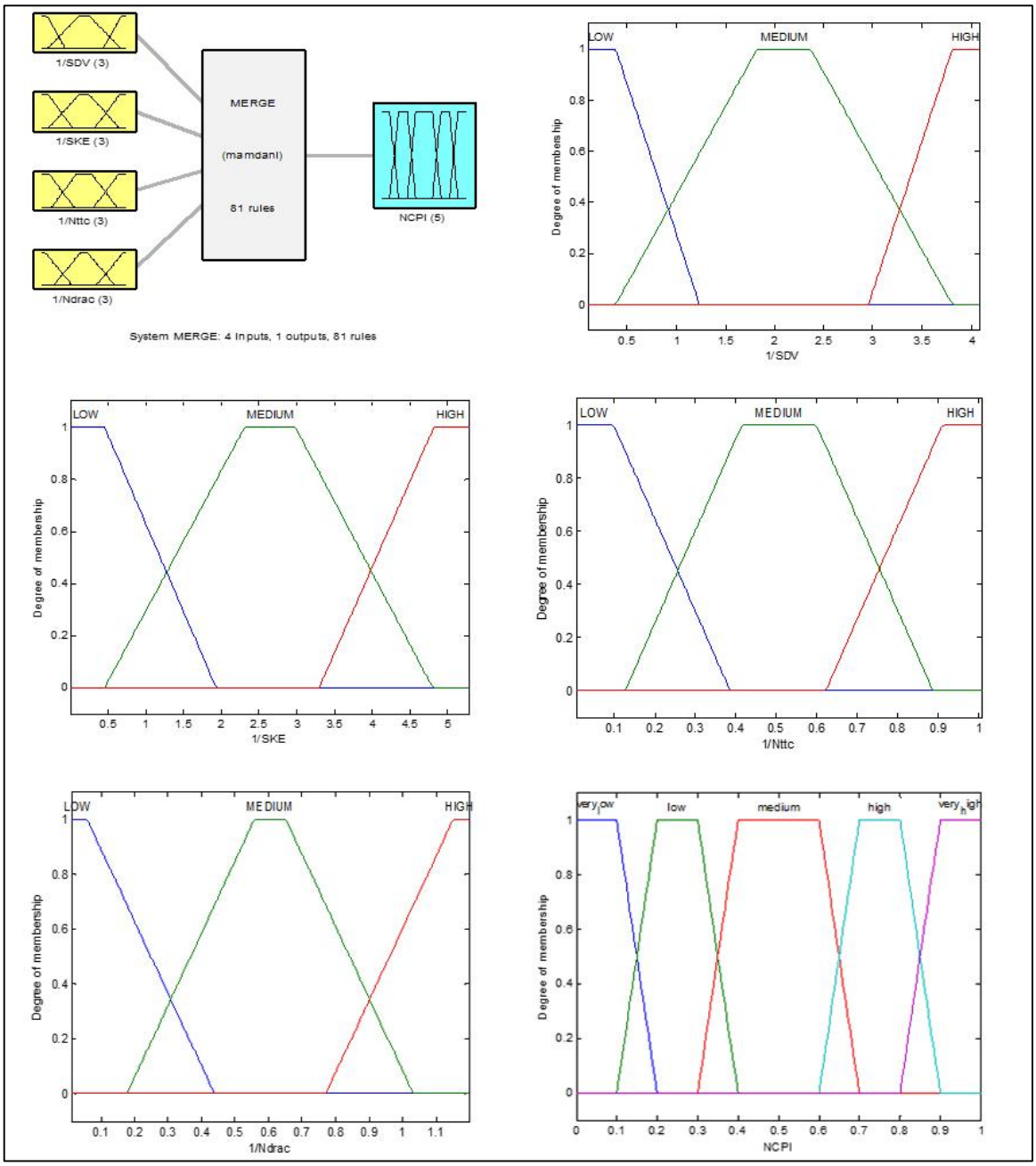

Figure 5. *FIS* structure and membership functions for *NCPI* and variables for merge areas

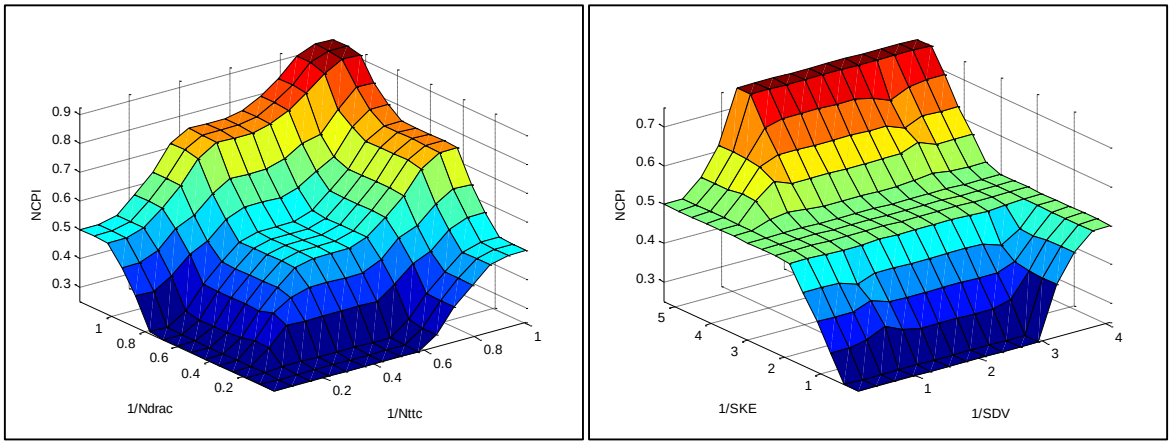

Figure 6. *NCPI* against number and severity variables for merge areas

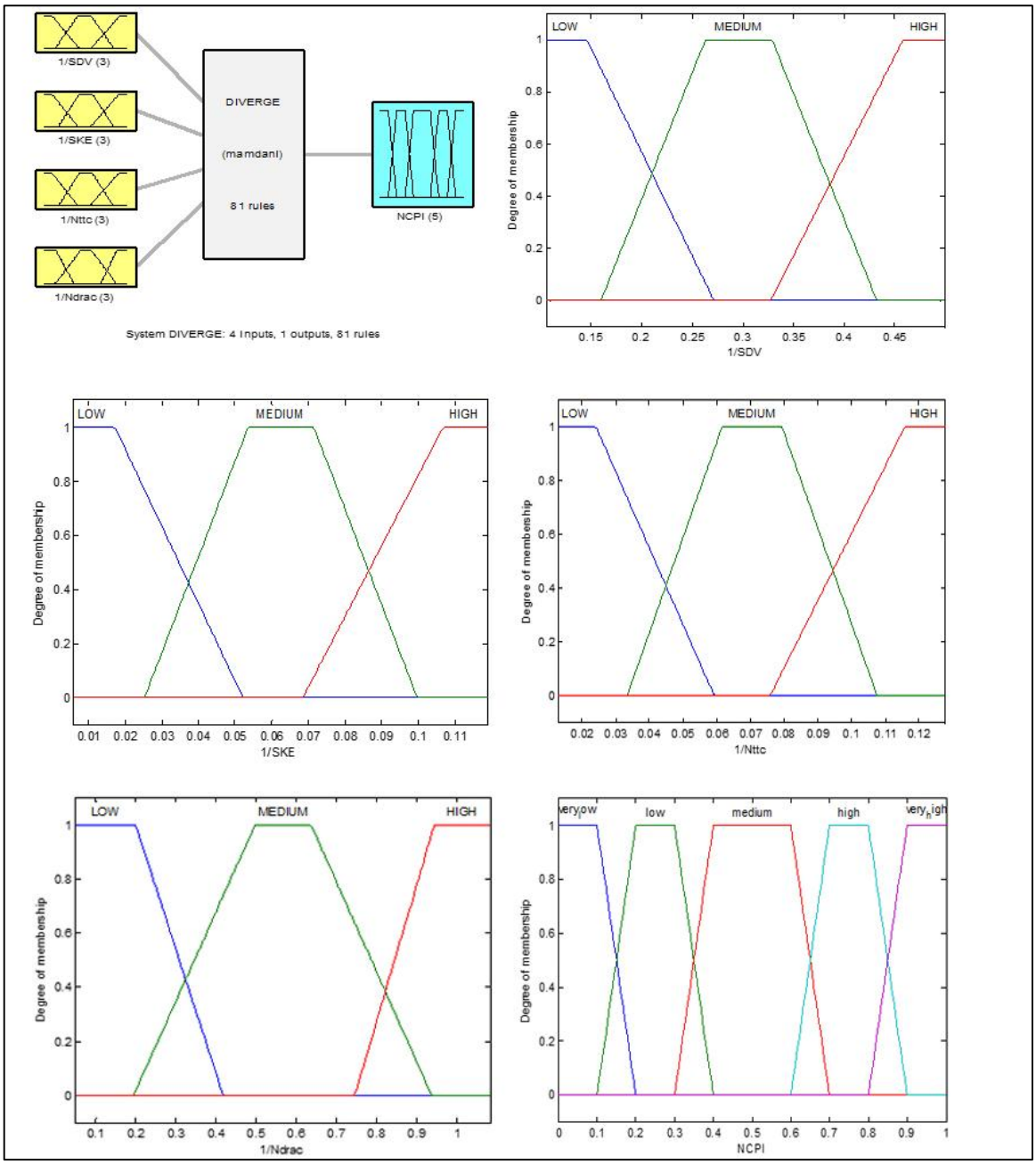

Figure 7. *FIS* structure and membership functions for *NCPI* and variables for diverge areas

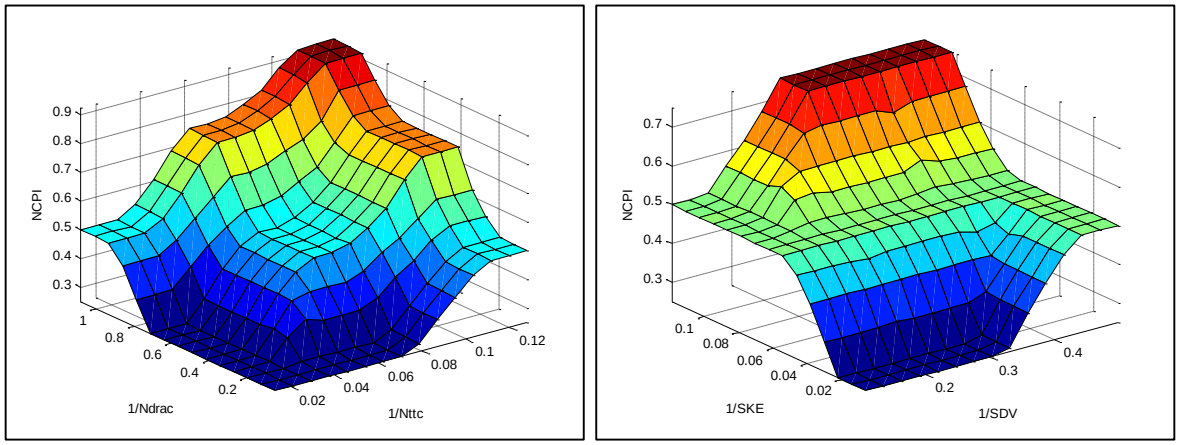

Figure 8. *NCPI* against number and severity variables for diverge areas

To recognize the effect of variation in the value of every geometric or traffic characteristic on *NCPI*, simulating different kinds of merge and diverge areas with different geometry and different traffic characteristic is a good strategy which solve the problem. Then *SL* or *NCPI* of merge and diverge areas could be determined based on trajectory data. Geometric and traffic characteristics of merge and diverge areas are effective variables in predicting *NCPI* indeed. These variables include length of acceleration lane, number of freeway lanes, number of lanes in on-ramp, freeway volume, on ramp volume, freeway free flow speed, and speed of on ramp for merge areas and length of deceleration lane, number of freeway lane, number of off ramp lanes, freeway volume, freeway free flow speed, and speed of off ramp for diverge areas. Tables 3 and 4 present variables description and their used ranged in simulation.

Table 3. Variables description and their used ranged in simulation for merge areas

Variables*	L_{ACC} (m)	V_{FW} (Veh/h)	N_{FW} #	$V_{R\text{-}ON}$ (Veh/h)	$N_{R\text{-}ON}$ #	S_{FW} (Km/h)	$S_{R\text{-}ON}$ (Km/h)
Range:	100 to 500	750 to 2970	3 to 4	600 to 1600	1 to 2	90 to 120	40 to 60

*L_{ACC} is length of acceleration lane, V_{FW} is freeway volume, N_{FW} is number of freeway lane, $V_{R\text{-}ON}$ is on ramp volume, $N_{R\text{-}ON}$ is number of on ramp lanes, S_{FW} is freeway free flow speed, $S_{R\text{-}ON}$ is speed of on ramp

Table 4. Variables description and their used ranged in simulation for diverge areas

Variables*	L_{DEC} (m)	N_{FW} #	$N_{R\text{-}OFF}$ #	V_{FW} (Veh/h)	S_{FW} (Km/h)	$S_{R\text{-}OFF}$ (Km/h)
Range:	100 to 500	3 to 4	1 to 2	750 to 2970	90 to 120	40 to 60

*L_{DEC} is length of deceleration lane, N_{FW} is number of freeway lane, $N_{R\text{-}OFF}$ is number of off ramp lanes, V_{FW} is freeway volume, S_{FW} is freeway free flow speed, $S_{R\text{-}OFF}$ is speed of off ramp

By combining different geometric and traffic characteristics of merge and diverge areas, 2160 different types of merge area and 720 different type of diverge areas were produced and simulated. *NCPI* of merge and diverge areas was calculated by analyzing trajectory data. 2160 rows of information for merge areas and 720 rows of information for diverge areas containing *NCPI* as function and the geometric and traffic characteristics as variables were produced after data analysis.

3.1. ANN

ANN was built by the rows of information. The properties of the *ANN* were as below:

Merge Area:
NO. of layers: 3
NO. of neurons in each layer: 7
Train data: 60 % of all data
Test data: 20 % of all data
Validation data: Remained data (20 % of all)
Training function: Trainlm
Function of hidden layers: Tansig
Function of output layer: Purelin

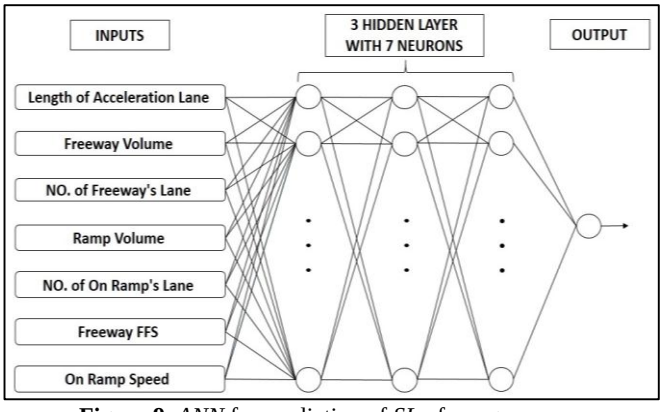

Figure 9. *ANN* for prediction of *SL* of merge area

Diverge Area:
NO. of layers: 3
NO. of neurons in each layer: 7
Train data: 60 % of all data
Test data: 20 % of all data
Validation data: Remained data (20 % of all)
Training function: Trainlm
Function of hidden layers: Tansig
Function of output layer: Purelin

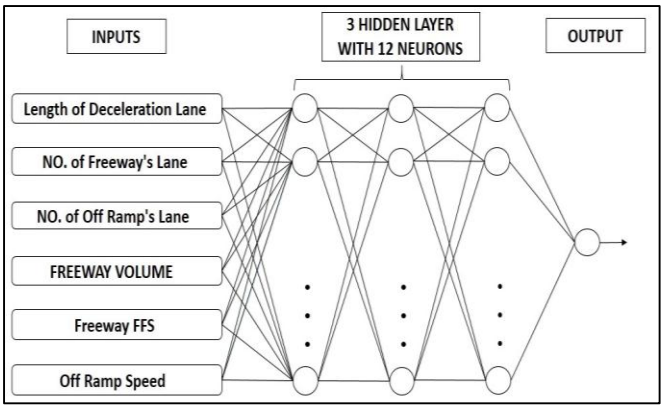

Figure 10. *ANN* for prediction of *SL* of diverge area

Number of layers, number of neurons, training functions, hidden layers, and output layer were determined after a lot of try and error attempts to reach minimum Root Mean Square Error (*RMSE*). By using this *ANN*, *SL* could be predicted in merge and diverge areas when there is enough information about the values of geometric and traffic characteristics of these areas.

3.2. PSO

To develop the models using *PSO* to predict *SL* of merge and diverge areas, a basic equation should be proposed. Constant parameters would be determined based on

information rows. The results of *NCPI* by this equation were compared with *NCPI* from the rows of information. The global best results of constant parameters will be obtained after several iterations to reach possible minimum *RMSE*. Some equations were proposed and after a lot of try and error attempts, Eq. (31) was considered for merge area and Eq.s (32) and (33) for diverge areas.

$$NCPI_M = b_1 \times 0.143^{b_2}|a_1 e^{a_2 L_{ACC}} + a_3 e^{a_4 L_{ACC}} + a_5 {V_{FW}}^{a_6} + a_7 N_{FW} + a_8 {V_{R-ON}}^{a_9} + a_{10} N_{R-ON} + a_{11} e^{a_{12} S_{FW}} + a_{13} e^{a_{14} S_{FW}} + a_{15} {S_{R-ON}}^{a_{16}} + a_{17}|^{b_2} + b_3 \quad (31)$$

$$NCPI_D = b_1 \tan|b_2\theta + b_3| + b_4 \quad (32)$$

$$\theta = 0.167(a_1 {L_{DEC}}^{a_2} + a_3 N_{FW} + a_4 N_{R-OFF} + a_5 {V_{FW}}^{a_6} + a_7 e^{a_8 S_{FW}} + a_9 S_{R-OFF} + a_{10}) \quad (33)$$

In which *NCPIM* is *SL* of merge area, *NCPID* is *SL* of diverge area, *LACC* is length of acceleration lane, *LDEC* is length of deceleration lane, *NFW* is number of on freeway lanes, *NR-ON* is number of on ramp lanes, *NR-OFF* is number of off ramp lanes, *VFW* is freeway volume, *VR-ON* is on ramp volume, *SFW* is freeway free flow speed, *SR-ON* is speed of on ramp, *SR-OFF* is speed of off ramp, and *ai* and *bi* are constant parameters.

3.3. Case Studies and Models Verification

Models should be verified by case studies. Survey results were compared with models outputs. With respect to possible difference between survey results and models outputs, it was necessary to determine that this difference was because of either data distribution and their random properties or a significant difference between the results. Statistical analysis shows whether there is significant difference between surveyed *SL* and corresponding *SL* predicted by models or not. Pooled t-test was used due to the limited number of samples. Statistical t could be calculated by Eq. (34)

$$t = (\mu_m - \mu_s){S_p}^{-1}({n_m}^{-1} + {n_s}^{-1})^{-0.5} \quad (34)$$

$$s_p = \left((n_m - 1){\sigma_m}^2 + (n_s - 1){\sigma_s}^2\right)^{0.5}(n_m + n_s - 2)^{-0.5} \quad (35)$$

in which μ_m and μ_s are mean of models population and mean of survey population, respectively. n_m and σ_m are number of samples and standard deviation of models results, respectively and n_s and σ_s are number of samples and standard deviation of survey results, respectively. Computed *t* should be compared with the tabulated values of t-distribution table. The tabulated values of t-distribution table depend on degree of freedom, *f*, which represents the number of independent parts. Degree of freedom is defined as Eq. (36) in t-distributions.

$$f = n_m + n_s - 2 \quad (36)$$

Once the statistical *t* is determined, the tabulated values of t-distribution table yield the probability of a t value being greater than the computed value. In order to limit the probability of a type I error to 0.05, the difference in the means will be considered significant only if the probability is less than or equal to 0.05, that is, if the calculated t value falls in the 5% area of the tail, or in other words, if there is less than a five percent chance that such a difference could be found in the same population.

If the probability is greater than 5% (or the computed t value is less than the tabulated values of t-distribution table) then such a difference in means could be found in the same population and the difference would be considered not significant. Table 5 shows tabulated values of t-distribution.

Table 5. t-Distribution table

df	p				
	0.900	**0.950**	**0.975**	**0.990**	**0.995**
1	3.078	6.314	12.706	31.820	63.657
2	1.886	2.920	4.303	6.965	9.925
3	1.638	2.353	3.182	4.541	5.841
4	1.533	2.132	2.776	3.747	4.604
5	1.476	2.015	2.571	3.365	4.032
6	1.440	1.943	2.447	3.143	3.707
7	1.415	1.895	2.365	2.998	3.499
8	1.397	1.860	2.306	2.897	3.355
9	1.383	1.833	2.262	2.821	3.250
10	1.372	1.812	2.228	2.764	3.169
11	1.363	1.796	2.201	2.718	3.106
12	1.356	1.782	2.179	2.681	3.055
13	1.350	1.771	2.160	2.650	3.012
14	1.345	1.761	2.145	2.625	2.977
15	1.341	1.753	2.131	2.602	2.947
16	1.337	1.746	2.120	2.584	2.921
17	1.333	1.740	2.110	2.567	2.898
18	1.330	1.734	2.101	2.552	2.878
19	1.328	1.729	2.093	2.539	2.861
20	1.325	1.725	2.086	2.528	2.845
21	1.323	1.721	2.080	2.518	2.831
22	1.321	1.717	2.074	2.508	2.819
23	1.319	1.714	2.069	2.500	2.807
24	1.318	1.711	2.064	2.492	2.797
25	1.316	1.708	2.060	2.485	2.787
26	1.315	1.706	2.056	2.479	2.779
27	1.314	1.703	2.052	2.473	2.771
28	1.313	1.701	2.048	2.467	2.763
29	1.311	1.699	2.045	2.462	2.756
30	1.310	1.697	2.042	2.457	2.750
31	1.309	1.695	2.040	2.453	2.744
32	1.309	1.694	2.037	2.449	2.738
33	1.308	1.692	2.035	2.445	2.733
34	1.307	1.691	2.032	2.441	2.728
35	1.306	1.690	2.030	2.438	2.724
36	1.306	1.688	2.028	2.434	2.719
37	1.305	1.687	2.026	2.431	2.715
38	1.304	1.686	2.024	2.429	2.712
39	1.304	1.685	2.023	2.426	2.708
40	1.303	1.684	2.021	2.423	2.704
42	1.302	1.682	2.018	2.418	2.698
44	1.301	1.680	2.015	2.414	2.692
46	1.300	1.679	2.013	2.410	2.687
48	1.299	1.677	2.011	2.407	2.682
50	1.299	1.676	2.009	2.403	2.678
60	1.296	1.671	2.000	2.390	2.660
70	1.294	1.667	1.994	2.381	2.648
80	1.292	1.664	1.990	2.374	2.639
90	1.291	1.662	1.987	2.369	2.632
100	1.290	1.660	1.984	2.364	2.626
120	1.289	1.658	1.980	2.358	2.617
150	1.287	1.655	1.976	2.351	2.609
200	1.286	1.652	1.972	2.345	2.601
300	1.284	1.650	1.968	2.339	2.592
500	1.283	1.648	1.965	2.334	2.586
∞	1.282	1.645	1.960	2.326	2.576

4. Results

Rows of information were generated after simulating and analyzing trajectory data. This rows of information contained seven traffic and geometric variables and one function of *NCPI* for merge areas and six traffic and geometric variables and one function of *NCPI* for diverge areas. *ANN* was developed by using this rows of information. *ANN* results for merge areas are illustrated in Figure 11 to Figure 19 and Table 6.

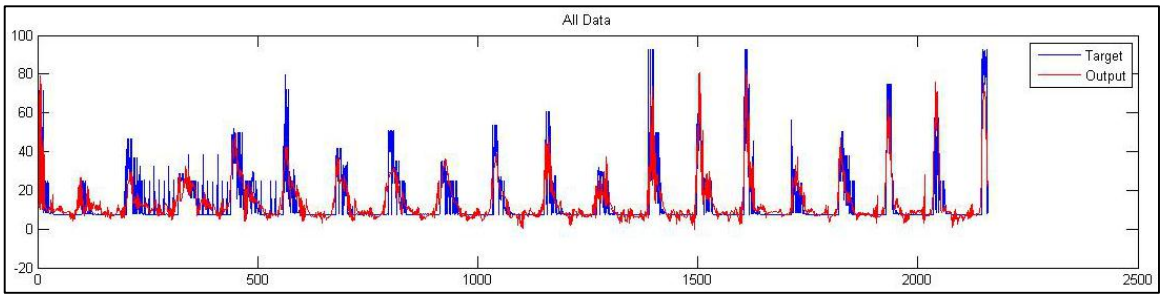

Figure 11. All data comparison of *ANN* output and *SL* in rows of information as target for merge area

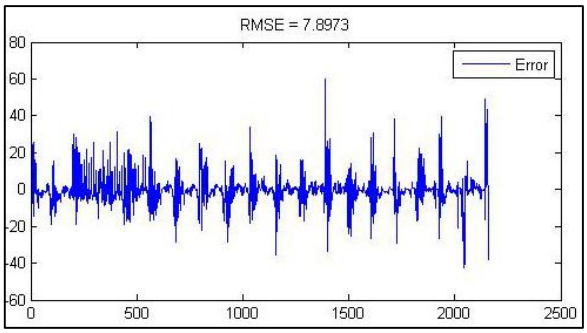

Figure 12. *All data error diagram for merge area*

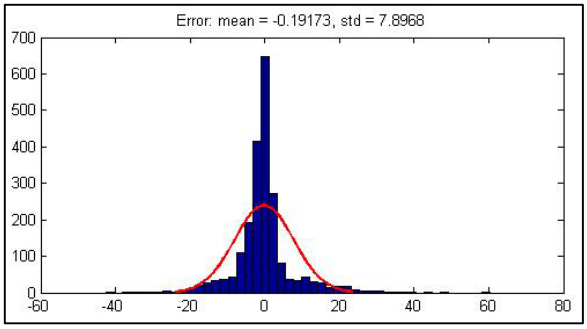

Figure 13. All data error distribution for merge area

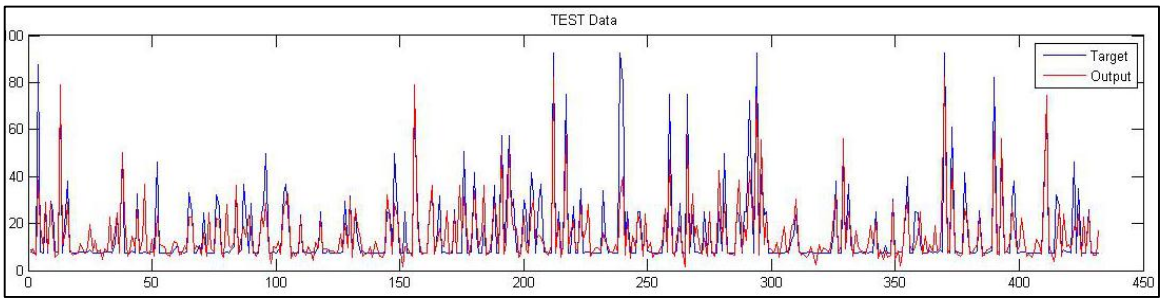

Figure 14. Test data comparison of *ANN* output and *SL* in rows of information as target for merge area

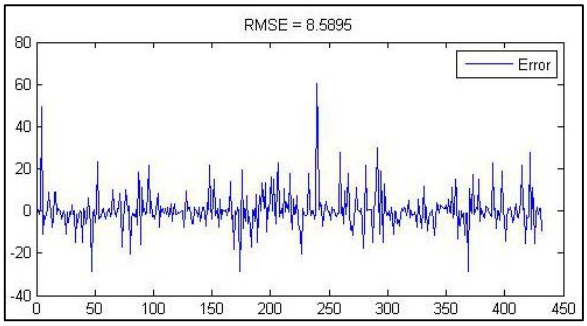

Figure 15. Test data error diagram for merge area

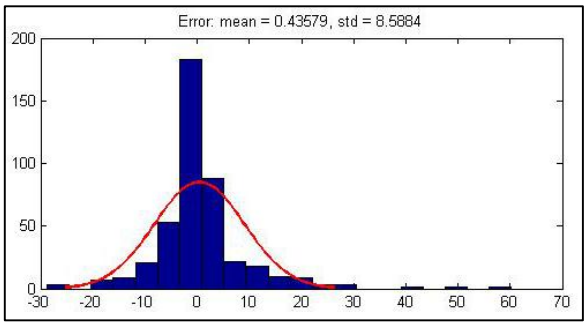

Figure 16. Test data error distribution for merge area

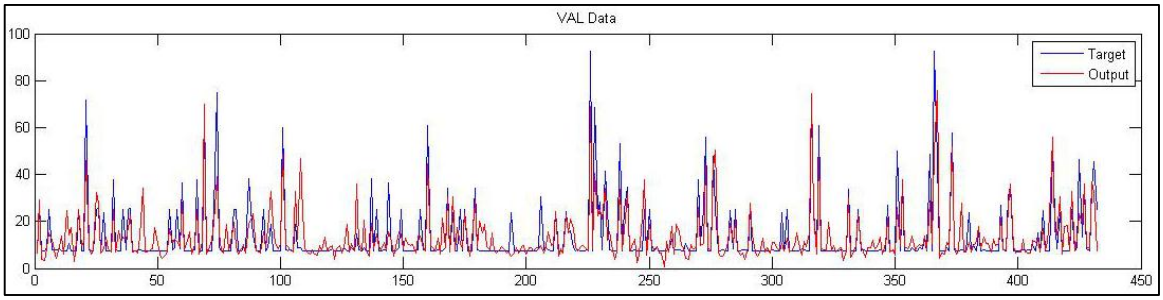

Figure 17. Validation data comparison of *ANN* output and *SL* in rows of information as target for merge area

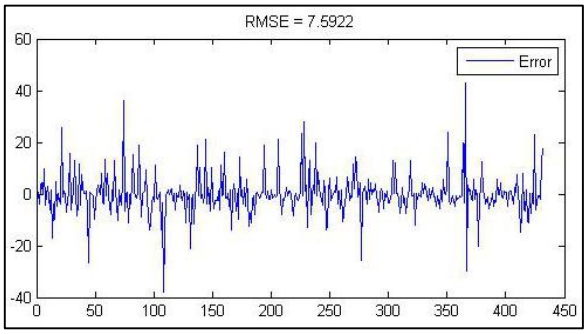

Figure 18. Validation data error diagram for merge area

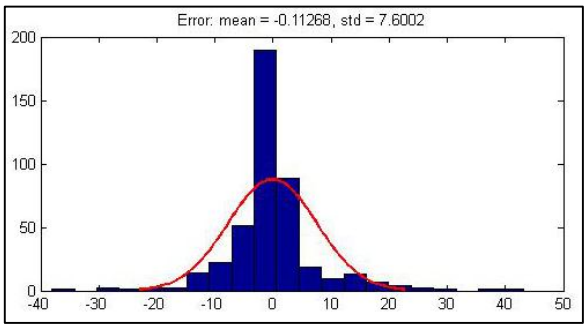

Figure 19. Validation data error distribution for merge area

Table 6. Accuracy of *ANN* outputs for all data for merge area

Standard deviation.	Error mean	*RMSE*
7.89	-0.191	7.89

ANN results for diverge areas are also presented in Figure 20 to Figure 28 and Table 7. Results were categorized in three collections of all data, test data, and validation data. For each collection, comparison between *ANN* outputs and *NCPI* in rows of information as target was described in first graph. Error diagram and error distribution of data of each collection were presented in second and third graph, respectively. Standard deviation, error mean, and RMSE of every collection are also mentioned in the graphs of each collection.

Standard deviation, error mean, and *RMSE* of three collections reflect a good development of models by *ANN*.

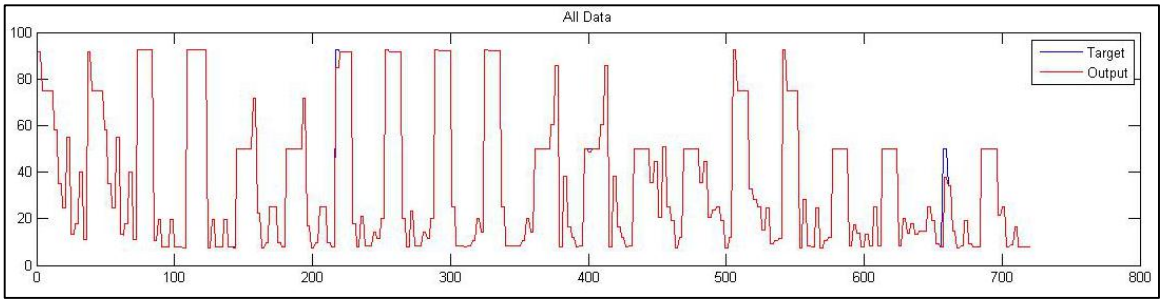

Figure 20. All data comparison of *ANN* output and *SL* in rows of information as target for diverge area

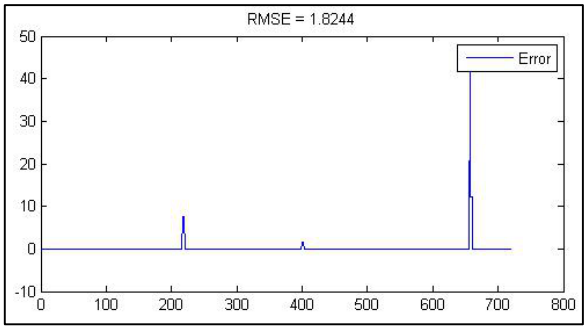

Figure 21. All data error diagram for diverge area

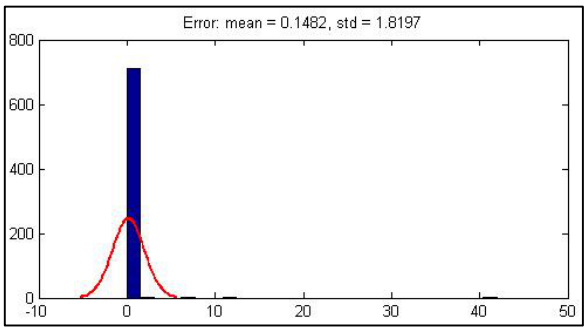

Figure 22. All data error distribution for diverge area

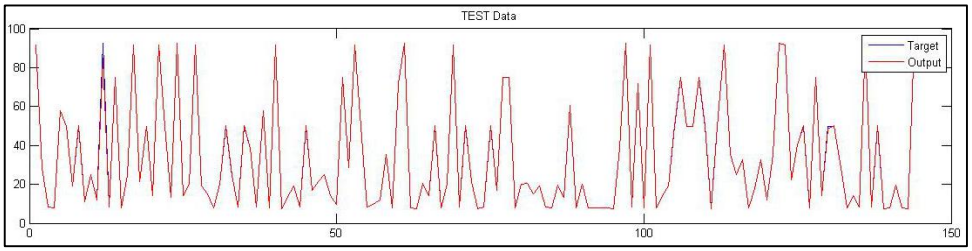

Figure 23. Test data comparison of *ANN* output and *SL* in rows of information as target for diverge area

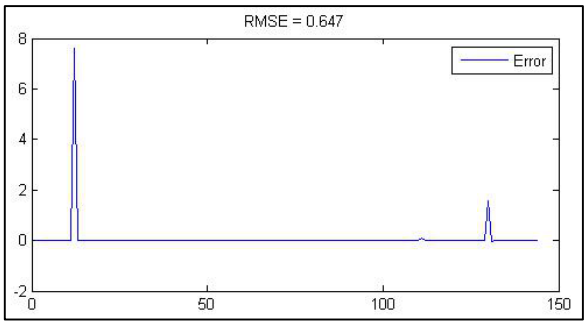

Figure 24. Test data error diagram for diverge area

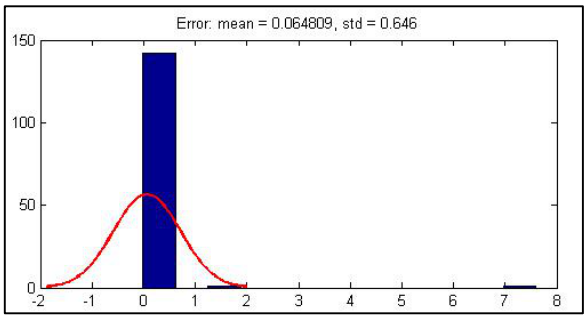

Figure 25. Test data error distribution for diverge area

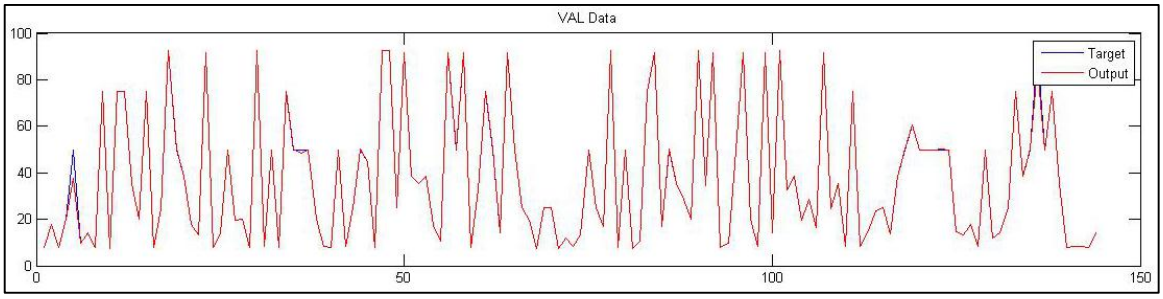

Figure 26. Validation data comparison of *ANN* output and *SL* in rows of information as target for diverge area

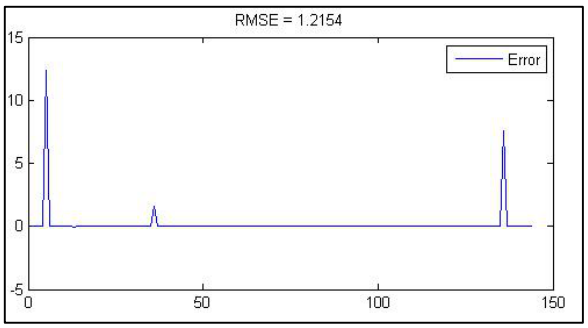

Figure 27. Validation data error diagram for diverge area

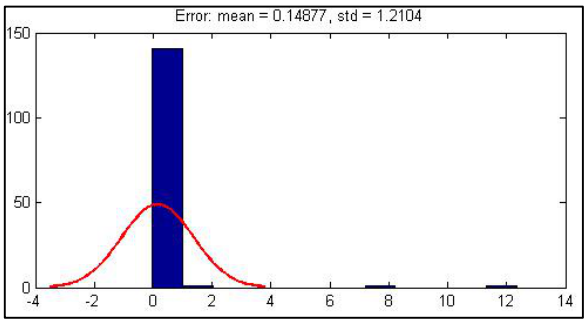

Figure 28. Validation data error distribution for diverge area

Table 7. Accuracy of ANN outputs for all data for diverge area

Standard deviation.	Error mean	*RMSE*
1.81	0.148	1.82

Constant parameters of Eq. (31) were also determined by using *PSO* algorithm. Results are represented in Figure 29 and Table 8 for merge areas.

Table 8. Constant parameters of Eq .(31) for merge area

a1	*a2*	*a3*	*a4*	*a5*	*a6*	*a7*	*MSE*	*RMSE*
0.6	-5.6	0	0.6	7	5.204	-30		
a8	*a9*	*a10*	*a11*	*a12*	*a13*	*a14*		
-210	-5.625	46.9	355320000000000	-1.2	69.564	0.302	184.245	13.57
a15	*a16*	*a17*		*b1*	*b2*	*b3*		
1800000	-14	0		0.428	0.0816	2.891		

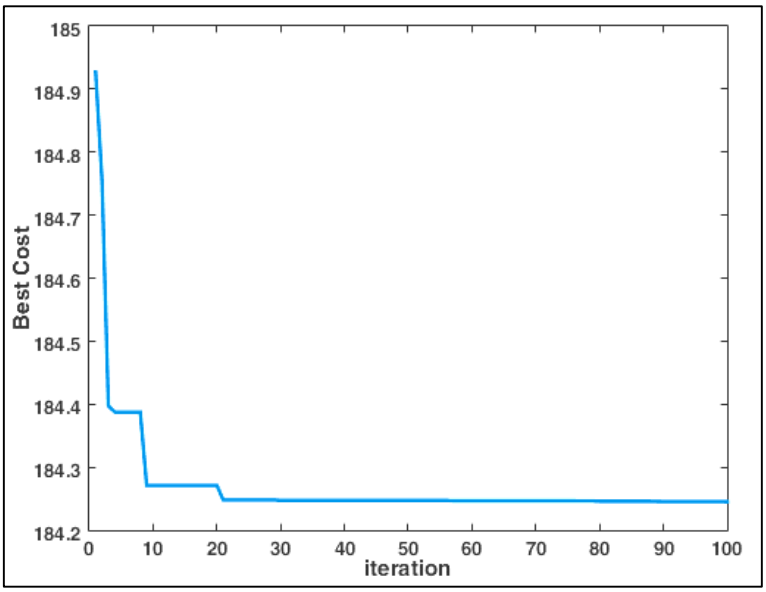

Figure 29. *PSO* iteration for merge area (Best Cost = MSE)

The value of *RMSE* showed good development of the model. Thus, the Eq. (31) could be rewritten as Eq. (37).

$$NCPI_M = 0.365\left|0.6\, e^{-5.6\, L_{ACC}} + 7\, {V_{FW}}^{5.204} - 30\, N_{FW} - 210\, {V_{R-ON}}^{-5.625} + 46.9\, N_{R-ON} + 3.55\times 10^{14}\, e^{-1.2 S_{FW}} + 69.564\, e^{0.302\, S_{FW}} + 1.8\times 10^{6}\, {S_{R-ON}}^{-14}\right|^{0.0816} + 2.891 \quad (37)$$

All parameters were described previously. Constant parameters of Eq.s (32) and (33) were also determined and shown in Figure 30 and Table 9 for diverge areas.

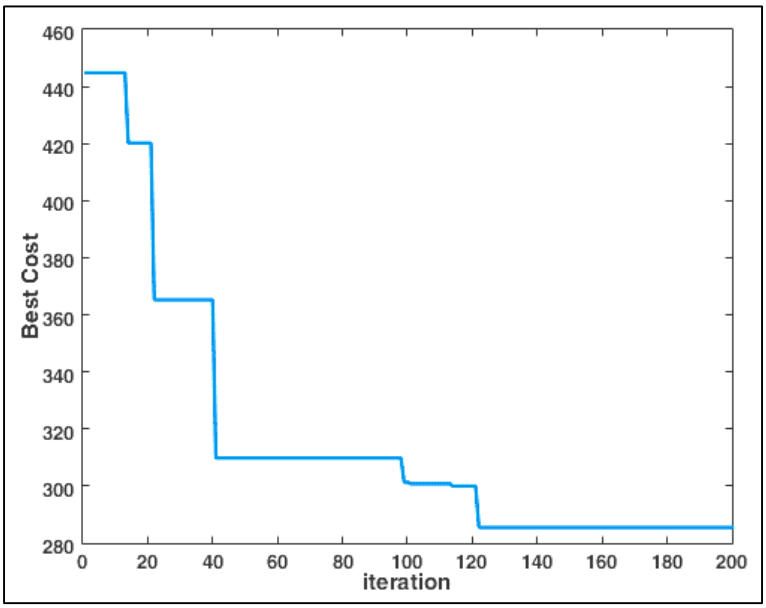

Figure 30. *PSO* iteration for diverge area (Best Cost = *MSE*)

Table 9. Constant parameters of Eq.s (32) and (33) for diverge area

a1	*a2*	*a3*	*a4*	*a5*	*a6*	*a7*	*MSE*	*RMSE*
-0.31	-0.32	29.97	15.56	-23.35	0.38	-135.92	285.49	16.90
a8	*a9*	*a10*	*b1*	*b2*	*b3*	*b4*		
-10.01	0.03	-910.00	-18.20	1.23	37.80	25.34		

The value of *RMSE* showed good development of the model. Thus, the Eq.s (32) and (33) could be rewritten as Eq.s (38) and (39).

$$NCPI_D = -18.2\, tan|1.23\,\theta + 37.80| + 25.34 \quad (38)$$

$$\theta = 0.167\big(-0.31\, {L_{DEC}}^{-0.32} + 29.97\, N_{FW} + 15.56\, N_{R-OFF} - 23.35\, {V_{FW}}^{0.38} - 135.92\, e^{-10.01\, S_{FW}} + 0.03\, S_{R-OFF} - 910\big) \quad (39)$$

All parameters were described previously. As it was mentioned before, case studies were used to verify the models. Figure 31 shows studied merge areas and traffic and geometric characteristics of them are presented in Table 10.

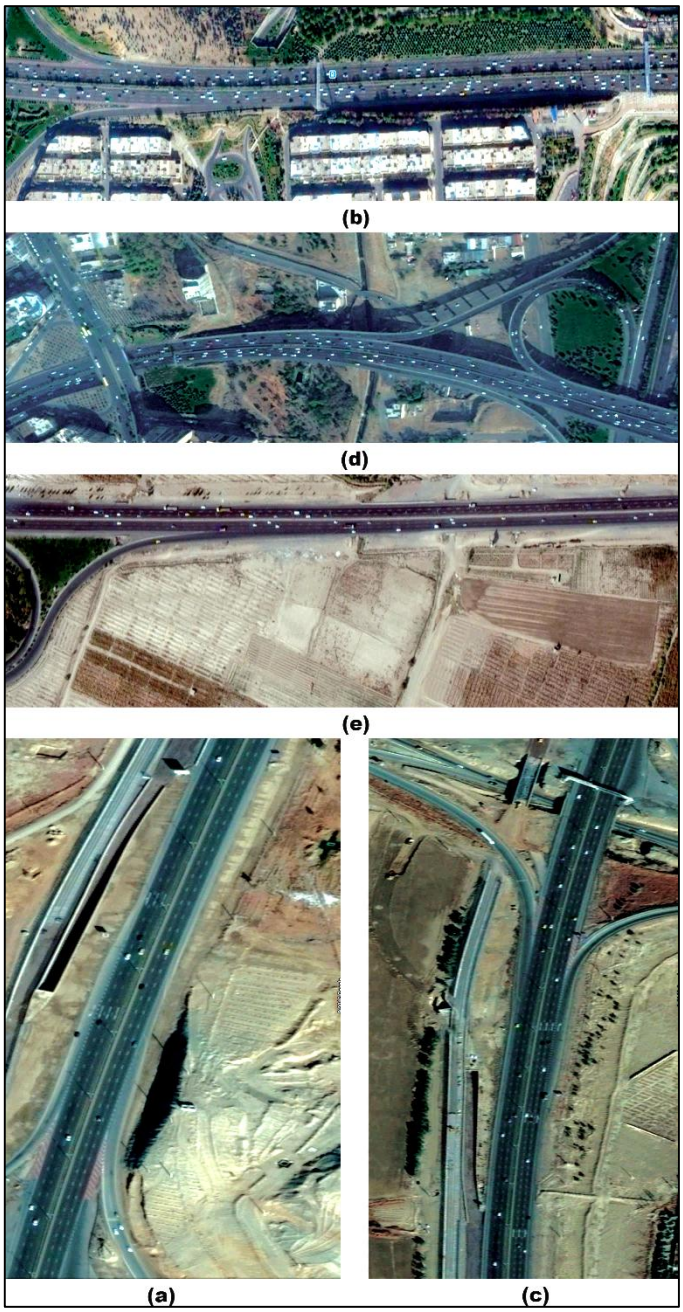

Figure 31. Case studies of merge areas: (a) Tehran-Qom Freeway S-N: Merge Vahnabad W, (b) Hemmat Freeway W-E: Merge Asharfi N, (c) Tehran-Qom Freeway N-S: Merge Vahnabad E, (d) Niayesh Freeway E-W: Merge Chamran S, (e) Tehran-Saveh Freeway W-E: Merge Shahriar W

Table 10. Characteristics of studied merge areas

Location:	Characteristics						
	L_{ACC} (m)	V_{FW} (veh/h)	N_{FW} (-)	V_{R-ON} (veh/h)	N_{R-ON} (-)	S_{FW} (km/h)	S_{R-ON} (km/h)
Hemmat Freeway W-E: MERGE Asharfi N	145	5023	4	1253	2	90	50
Niayesh Freeway E-W: MERGE Chamran S	118	3794	3	909	2	80	40
Tehran-Qom Freeway N-S: MERGE Vahnabad E	173	2252	3	169	1	120	60
Tehran-Qom Freeway S-N: MERGE Vahnabad W	154	1266	3	440	1	120	60
Tehran-Saveh Freeway W-E:MERGE Shahriar W	225	2667	3	361	2	120	40

The values of *NCPI* were predicted by applying two developed models on studied merge areas with characteristics presented in Table 10. Results of statistical analysis between means of *NCPI* predicted by both models versus *NCPI* surveyed in case studies are represented in Table 11 for merge areas.

Table 11. Results of statistical analysis between means of *NCPI* predicted by both models versus *NCPI* surveyed for merge areas

Location	*n*	*NCPI*						Statistical Pooled t-test					
		ANN Results		*PSO* Results		Survey Results							
		μ_m	σ_m	μ_m	σ_m	μ_s	σ_s	*f*	*t* (t-dist. table)	$S_{p\text{-}ANN}$	$S_{p\text{-}PSO}$	t_{ANN}	t_{PSO}
Hemmat Freeway W-E: MERGE Asharfi N	11	16.3381	2.18	18.85	4.21	17.20	2.12	20	1.725	2.15	3.33	0.94	1.16
Niayesh Freeway E-W: MERGE Chamran S	14	14.7116	3.09	17.06	5.11	15.59	3.12	26	1.706	3.10	4.23	0.75	0.92
Tehran-Qom Freeway N-S: MERGE Vahnabad E	25	16.1305	4.48	14.41	5.30	15.73	4.21	48	1.687	4.35	4.79	0.33	0.97
Tehran-Qom Freeway S-N: MERGE Vahnabad W	19	15.2322	2.28	13.01	3.12	14.53	2.03	36	1.692	2.16	2.64	1.00	1.78
Tehran-Saveh Freeway W-E: MERGE Shahriar W	18	18.1533	3.41	15.17	4.22	17.24	3.07	34	1.694	3.25	3.69	0.85	1.68

It could be found that there are no significant differences between means of *NCPI* for models population and real population in merge areas when almost all computed statistical t presented in Table 11 (which are achieved from statistical analysis of population of models and studied areas) are less than the tabulated values of t-distribution table. Figure 32 shows studied diverge areas and traffic and geometric characteristics of them are presented in Table 12.

Figure 32. Case studies of diverge areas: (a) Yadegar Freeway N-S: Diverge Kouhestan E, (b) Tehran-Saveh Freeway E-W: Diverge Dehshade W, (c) Tehran-Saveh Freeway E-W: Diverge Robatkarim E, (d) Hakim Freeway W-E: Diverge Sheikh Bahaee S, (e) Hemmat Freeway W-E: Diverge YADEGAR S

Table 12. Characteristics of studied diverge areas

Location	Characteristics					
	L_{DEC} (m)	N_{FW} (-)	$N_{R\text{-}OFF}$ (-)	V_{FW} (veh/h)	S_{FW} (km/h)	$S_{R\text{-}OFF}$ (km/h)
Hakim Freeway W-E: DIVERGE Sheikh Bahaee S	172	4	1	3188	80	30
Hemmat Freeway W-E: DIVERGE Yadegar S	202	4	2	4196	80	60
Tehran-Saveh Freeway E-W: DIVERGE Dehshade W	215	3	2	4160	120	60
Tehran-Saveh Freeway E-W: DIVERGE Robatkarim E	180	3	2	1895	120	40
Yadegar Freeway N-S: DIVERGE Kouhestan E	152	3	1	1930	80	50

The values of *NCPI* were predicted by applying two developed models on studied diverge areas with characteristics presented in Table 12. Results of statistical analysis between means of *NCPI* predicted by both models versus *NCPI* surveyed in case studies are represented in Table 13 for diverge areas.

Table 13. Results of statistical analysis between means of NCPI predicted by both models versus NCPI surveyed for diverge areas

Location	n	*NCPI*						Statistical Pooled t-test					
		ANN Results		PSO Results		Survey Results							
		μ_m	σ_m	μ_m	σ_m	μ_s	σ_s	f	t (t-dist. table)	$S_{p\text{-}ANN}$	$S_{p\text{-}PSO}$	t_{ANN}	t_{PSO}
Hakim Freeway W-E: DIVERGE Sheikh Bahaee S	17	1.63936	0.18	1.61	0.20	1.65	0.20	32	1.694	0.19	0.20	0.18	0.66
Hemmat Freeway W-E: DIVERGE Yadegar S	13	32.3352	6.01	36.52	7.30	33.83	6.76	24	1.711	6.39	7.03	0.60	0.98
Tehran-Saveh Freeway E-W: DIVERGE Dehshade W	22	49.5555	8.72	57.17	10.86	52.18	9.91	42	1.681	9.34	10.40	0.93	1.59
Tehran-Saveh Freeway E-W: DIVERGE Robatkarim E	14	5.6069	1.83	4.23	1.44	5.39	1.83	26	1.706	1.83	1.65	0.32	1.86
Yadegar Freeway N-S: DIVERGE Kouhestan E	9	89.363	14.66	99.00	17.63	92.65	16.50	16	1.746	15.61	17.07	0.45	0.79

It could be found that there are no significant differences between means of *NCPI* for models population and real population in diverge areas when almost all computed statistical t presented in Table 13 (which are achieved from statistical analysis of population of models and studied areas) are less than the tabulated values of t-distribution table.

5. Conclusion

The influence of variations of traffic and geometric characteristics of merge and diverge areas on *SL* of these areas were assessed in this paper. A model by *ANN* and another one by *PSO* algorithm were developed to predict SL of each merge and diverge area by defining *NCPI*. The results indicated good accuracy of models in terms of compliance with rows of information obtained from simulations and also surveyed data of case studies. The results also showed that in most cases results of model using *ANN* have more accuracy than the results of model using *PSO* algorithm. However, the advantage of using *PSO* algorithm is that finally, there will be certain relationship that can be conveniently used. While the model developed by *ANN* will not work when there is no database.

It should be noted that in general the proposed models will be valid when the geometric and traffic characteristics of studied areas are in the range of variables values used in model development. Obviously, the more distance between the values of these characteristics and the range of mentioned variables values, the more reduction in validity of models. Another conclusion is that models could be developed to predict other traffic or safety criteria of merge and diverge areas or other traffic facilities based on their traffic and geometric characteristics using *ANN* and *PSO* algorithm.

References

[1] J. Xie, , Y. Ma, L. Yuan, P. Zhang, Y. Liu,. Safety and Capacity Performances of Single-lane Right Exit Ramp on Freeway: A Case Study in Jiangsu Province, China. Procedia Engineering, 137 (2016) 563–570.

[2] D. Eustace, A. Aylo, W. Y. Mergia,. Crash frequency analysis of left-side merging and diverging areas on urban freeway segments – A case study of I-75 through downtown Dayton, Ohio. Transportation Research Part C: Emerging Technologies 50 (2015) 78–85.

[3] H. Chen, H. Zhou , J. Zhao, P. Hsu, Safety performance evaluation of left-side off-ramps at freeway diverge areas. Accident Analysis & Prevention 43 (2011) 605–612.

[4] W. Y. Mergia, D. Eustace, D. Chimba, M. Qumsiyeh, Exploring factors contributing to injury severity at freeway merging and diverging locations in Ohio. Accident Analysis & Prevention 55 (2013) 202–210.

[5] M. SARVI, Using Modeling and Micro-Simulation Approaches to Develop Control Strategies for Congested Freeway Merging points Considering Safety Aspects. Paper presented at the 1st International Conference on Traffic Accident, Tehran, Iran, (2005).

[6] B. Lu, , L. Zhibin, D. Muqing, W. Wei, L. Pan, Analysis of Crash Risks by Collision Type at Freeway Diverge Area Using Multivariate Modeling Technique, (2015).

[7] V. Kiattikomol, A. Chatterjee, J. E. Hummer, M. S. Younger, Planning Level Regression Models for Prediction of Crashes on Interchange and Noninterchange Segments of Urban Freeways. Journal of Transportation Engineering 134 (2008).

[8] K. Jetto, H. Ez-Zahraouy, A. Benyoussef,. An investigation of merging and diverging cars on a multi-lane road using a cellular automation model. Chinese Physics B 21 (2012) 118901.

[9] M. Sarhan, , Y. Hassan, A. O. Abd El Halim, Safety performance of freeway sections and relation to length of

[10] J. Hayward, Near misses as a measure of safety at urban intersections. (PHD), The Pennsylvania State University, University Park, Pennsylvania State, (1971).

[11] K. Vogel, A comparison of headway and time to collision as safety indicators. Accident Analysis & Prevention 35 (2003), 427–433.

[12] M. M. Minderhoud, P. H. L. Bovy, Extended time-to-collision measures for road traffic safety assessment. Accident Analysis & Prevention 33 (2001) 89–97.

[13] J. Archer, Indicators for traffic safety assessment and prediction and their application in micro-simulation modelling: A study of urban and suburban intersections. (PHD), Royal Institute of Technology, Stockholm, Sweden, (2005).

[14] A. Sobhani, W. Young, D. Logan, S. Bahrololoom, A kinetic energy model of two-vehicle crash injury severity. Accident Analysis & Prevention 43 (2011) 741–754.

[15] D. Gettman, L. Head, Surrogate safety measures from traffic simulation models, 2003.

[16] H. Behbahani, N. Nadimi, A framework for applying surrogate safety measures for sideswipe conflicts. speed-change lanes. Canadian Journal of Civil Engineering 35 (2008) 531–541.
International Journal for Traffic & Transport Engineering 5 (2015).

[17] H. Behbahani, , N. Nadimi, S. S. Naseralavi, New time-based surrogate safety measure to assess crash risk in car-following scenarios. Transportation Letters, 7 (2015) 229–238.

[18] S. Hirst, R. Graham, The format and presentation of collision warnings. Ergonomics and safety of intelligent driver interfaces, (1997).

[19] J. H. Hogema, W. H. Janssen, Effects of intelligent cruise control on driving behavior (TM-1996-C-12), (1996).

[20] A.Van der Horst, A Time-Based Analysis of Road User Behavior in Normal and Critical Encounters. Paper presented at the TNO Institute for Perception, Soesterberg, Netherlands, (1990).

[21] A. K. Maurya, P. S. Bokare, Study of deceleration behaviour of different vehicle types, International Journal for Traffic and Transport Engineering 2 (2012) 253–270.

[22] AASHTO, Highway Safety Manual, 1st Edition, 2010.